Acta Pharmaceutica Sinica B 2022;12(7):3167–3176

Chinese Pharmaceutical Association
Institute of Materia Medica, Chinese Academy of Medical Sciences

Acta Pharmaceutica Sinica B

www.elsevier.com/locate/apsb
www.sciencedirect.com

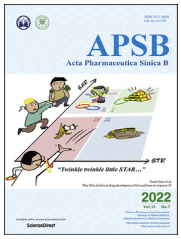

ORIGINAL ARTICLE

Metabolic engineering of yeasts for green and sustainable production of bioactive ginsenosides F2 and 3β,20*S*-Di-*O*-Glc-DM

Fenglin Jiang, Chen Zhou, Yan Li, Haidong Deng, Ting Gong, Jingjing Chen, Tianjiao Chen, Jinling Yang*, Ping Zhu*

State Key Laboratory of Bioactive Substance and Function of Natural Medicines, NHC Key Laboratory of Biosynthesis of Natural Products, CAMS Key Laboratory of Enzyme and Biocatalysis of Natural Drugs, Institute of Materia Medica, Chinese Academy of Medical Sciences & Peking Union Medical College, Beijing 100050, China

Received 20 January 2022; received in revised form 27 March 2022; accepted 15 April 2022

KEY WORDS

Ginsenoside;
UDP-glycosyltransferase;
Metabolic engineering;
Synthetic biology;
Saccharomyces cerevisiae;
CRISPR/Cas9 system;
Microbial cell factory;
Anti-pancreatic cancer activity

Abstract Both natural ginsenoside F2 and unnatural ginsenoside 3β,20*S*-Di-*O*-Glc-DM were reported to exhibit anti-tumor activity. Traditional approaches for producing them rely on direct extraction from *Panax ginseng*, enzymatic catalysis or chemical synthesis, all of which result in low yield and high cost. Metabolic engineering of microbes has been recognized as a green and sustainable biotechnology to produce natural and unnatural products. Hence we engineered the complete biosynthetic pathways of F2 and 3β,20*S*-Di-*O*-Glc-DM in *Saccharomyces cerevisiae via* the CRISPR/Cas9 system. The titers of F2 and 3β,20*S*-Di-*O*-Glc-DM were increased from 1.2 to 21.0 mg/L and from 82.0 to 346.1 mg/L at shake flask level, respectively, by multistep metabolic engineering strategies. Additionally, pharmacological evaluation showed that both F2 and 3β,20*S*-Di-*O*-Glc-DM exhibited anti-pancreatic cancer activity and the activity of 3β,20*S*-Di-*O*-Glc-DM was even better. Furthermore, the titer of 3β,20*S*-Di-*O*-Glc-DM reached 2.6 g/L by fed-batch fermentation in a 3 L bioreactor. To our knowledge, this is the first report on demonstrating the anti-pancreatic cancer activity of F2 and 3β,20*S*-Di-*O*-Glc-DM, and achieving their *de novo* biosynthesis by the engineered yeasts. Our work presents an alternative approach to produce F2 and 3β,20*S*-Di-*O*-Glc-DM from renewable biomass, which lays a foundation for drug research and development.

*Corresponding authors. Tel.: +86 10 63165199, +86 10 63165197.
E-mail addresses: yangjl@imm.ac.cn (Jinling Yang), zhuping@imm.ac.cn (Ping Zhu).

Peer review under responsibility of Chinese Pharmaceutical Association and Institute of Materia Medica, Chinese Academy of Medical Sciences.

https://doi.org/10.1016/j.apsb.2022.04.012

1. Introduction

Panax ginseng, known as the king of herbs, is famous for its excellent performance in the medicines and dietary supplements. Ginsenosides are the major active components of *P. ginseng*, which possess a wide range of pharmacological activities, including but not limited to anti-tumor, anti-aging, immunomodulation and neuroprotection[1,2]. Ginsenoside F2 exhibits anti-glioma[3], anti-breast cancer[4] and anti-gastric cancer[5] activities, but it is a trace component whose content is less than 0.01% in ginseng. Unnatural ginsenoside 3β,20*S*-Di-*O*-Glc-DM displays cytotoxicity against cancer cell lines, but until now it can only be produced by *in vitro* enzymatic reaction with a UDP-glycosyltransferase UGT109A1 from *Bacillus subtilis*[6]. Traditional methods for producing ginsenosides usually rely on direct extraction from *P. ginseng*, chemical synthesis and *in vitro* enzymatic catalysis. However, the scarcity of natural resources, long cultivation period (5−7 years) required for the growth of qualified roots, the continuous cropping obstacle of *P. ginseng*, low content and complicated extraction-separation processes of ginsenosides limit their direct extraction from *P. ginseng*. Although ginsenosides can be chemically synthesized, their complex structures and especial difficulty in stereoselective/stereospecific glycosylation make their chemical synthesis commercially infeasible[7]. Furthermore, the approach of *in vitro* enzymatic catalysis still requires expensive substrates to produce target ginsenosides[6]. Therefore, an economical approach for the large-scale production of F2 and 3β,20*S*-Di-*O*-Glc-DM is highly expected.

To date, the biosynthetic pathways of many medicinal natural products have been introduced into *Saccharomyces cerevisiae*, and the resultant engineered strains have been used as yeast cell factories for producing these products[8,9]. This approach can not only ensure the continuous acquisition of natural products from renewable biomass, but also protect natural resources and environment. Hence it has been acknowledged as a green and sustainable method for cost-effective production of natural products. Many natural medicines or their precursors have been produced with high yields in microbial cell factories, such as artemisinic acid, miltiradiene, taxadiene and so on[10−17]. Especially, the identification of genes involved in the biosynthetic pathways of ginsenosides, along with the rapid progress in synthetic biology tools, has contributed to the construction of a growing number of yeast cell factories for producing ginsenosides[18]. Compound K is the first ginsenoside biosynthesized in the engineered yeast[19]. The titer of compound K reached 5.0 g/L in a 5 L bioreactor by engineering yeast subcellular compartments[20]. The highest compound K titer of 5.74 g/L in a 1.3 L bioreactor was achieved by optimizing UGTPg1 expression and improving UDP-glucose (UDPG) supply[21]. A yeast cell factory producing 2.25 g/L ginsenoside Rh2 in a 10 L bioreactor was built by improving the C3−OH glycosylation efficiency and optimizing cytochrome P450 (CYP450) expression level[22]. The yeast strain producing ginsenoside Rg1 was constructed and further optimized by systematic engineering strategies and the titer of Rg1 reached 1.95 g/L in a 1.3 L bioreactor[23].

The construction of microbial cell factories can provide an alternative approach for the mass production of F2 and 3β,20*S*-Di-*O*-Glc-DM, but it has not been reported until now. In this study, we first constructed the biosynthetic pathways of F2 and 3β,20*S*-Di-*O*-Glc-DM in *S. cerevisiae*. Subsequently, we applied multistep metabolic engineering strategies to increase the titers of F2 and 3β,20*S*-Di-*O*-Glc-DM, including: (1) tuning the promoters of protopanaxadiol synthase (PPDS) and *Arabidopsis thaliana* NADPH-cytochrome P450 reductase 2 (ATR2) to make more carbon flux flow to protopanaxadiol (PPD), (2) screening high-efficiency C3-glycosyltransferase, (3) enhancing the supply of glycosyl receptors and overexpressing the transcriptional activators, (4) overexpressing the key genes involved in the glycosyl donor UDPG biosynthesis. These efforts led to the titers of 21.0 mg/L F2 and 346.1 mg/L 3β,20*S*-Di-*O*-Glc-DM at shake flask level. We further demonstrated that both F2 and 3β,20*S*-Di-*O*-Glc-DM exhibited anti-pancreatic cancer activity and the activity of 3β,20*S*-Di-*O*-Glc-DM was even better. Finally, the titer of 3β,20*S*-Di-*O*-Glc-DM reached 2.6 g/L by fed-batch fermentation in a 3 L bioreactor. This work provides a green and sustainable approach for producing F2 and 3β,20*S*-Di-*O*-Glc-DM from renewable biomass.

2. Materials and methods

2.1. Chemicals

Standard dammarenediol-II (DM), PPD, ginsenosides F2, compound K and Rh2 were purchased from Sigma−Aldrich Co. Ltd. (USA). 3β,20*S*-Di-*O*-Glc-DM, 3β-*O*-Glc-DM and 20*S*-*O*-Glc-DM were obtained by *in vitro* enzymatic reactions of DM catalyzed by UGT109A1, PgUGT74AE2 and UGTPg1, respectively[6,24].

2.2. Construction of plasmids

The gene expression cassettes of *DS-GFP*, *PgUGT74AE2*, *UGTPg1*, *tHMG1*, *IDI1*, *ERG20*, *ERG9*, *ERG1*, *ERG7* and *HAC1* were constructed in our previous work[24]. The genes (*INO2*, *PGM1*, *PGM2*, *UGP1*), the promoters (*ENO2*, *TEF2*) and the terminators (*FBA1*, *IDP1*) from *S. cerevisiae* were all synthesized by GenScript (Nanjing, China). The genes *M7* (mutant of *UGT74AC1*) from *Siraitia grosvenorii*[25], *UGTPn50-HV* (mutant of *UGTPn50*) from *Panax notoginseng*[22], *M7-1* (mutant of *UGT51*) from *S. cerevisiae*[26] and *UGT109A1* from *B. subtilis*[6] were all codon-optimized and synthesized. The ergosteryl-β-glucosidase (EGH1) gene was amplified from the genomic DNA of *S. cerevisiae* YPH499. Construction of integration modules were performed as our previous methods[24]. The plasmids harboring the integration modules are listed in Supporting Information Table S1.

2.3. In vitro UDP-glycosyltransferase activity assays

Heterologous expression of PgUGT74AE2 and UGTPg1 in *Escherichia coli* BL21 (DE3), enzymatic assays and identification of the target products were carried out as described previously[24].

2.4. Construction and optimization of the engineered yeasts

To construct ginsenoside F2-producing strain, the gene expression cassettes of *tHMG1*, *DS-GFP*, *PPDS*, *ATR2*, *PgUGT74AE2*, *UGTPg1* and *HIS* (Supporting Information Fig. S1) together with plasmid p-Cas9-gRNA were co-transformed into the δ1 site of Y-ΔHXK2[24]. A total of 10 single colonies were randomly picked from SD-HIS-URA plates and cultivated in YPD medium for 3 days to compare their titers of F2. The strain with the highest titer of F2 was named as YF2 (Table 1). Then, the promoters of *PPDS* and *ATR2* were adjusted. In the strain YF2, the expression cassettes of *PPDS* and *ATR2* were P_{PYK1}-*PPDS*-T_{ADH2} and P_{TDH3}-*ATR2*-T_{TPI1}. They were replaced by the expression cassettes

P_{TDH3}-*PPDS*-T_{ADH2} and P_{PYK1}-*ATR2*-T_{TPI1}, P_{TDH3}-*PPDS*-T_{ADH2} and P_{TEF2}-*ATR2*-T_{TPI1} to construct the strains YF2-B and YF2-C, respectively (Table 1). YF2, YF2-B and YF2-C were cultivated in triplicate to compare their titers of F2. The strain YF2-C with the highest titer of F2 was selected for further engineering.

Similarly, the 3*β*,20*S*-Di-*O*-Glc-DM-producing strain was constructed by transforming the expression cassettes of *tHMG1*, *DS-GFP*, *PgUGT74AE2*, *UGTPg1* and *HIS* (Supporting Information Fig. S2) together with plasmid p-Cas9-gRNA into the *δ*1 site of Y-ΔHXK2. Among 10 single colonies picked from SD-HIS-URA plates, the one with the highest titer of 3*β*,20*S*-Di-*O*-Glc-DM was named as YDP (Table 1). Then *PgUGT74AE2* was replaced by other C3-glycosyltransferase genes encoding M7 from *S. grosvenorii*, UGTPn50-HV from *P. notoginseng*, M7-1 from *S. cerevisiae* and UGT109A1 from *B. subtilis* (Fig. S2). The resultant strains with the highest titer of 3*β*,20*S*-Di-*O*-Glc-DM in each group were named as YDS, YDN, YDC and YDB, respectively (Table 1). The strain YDB did not harbor *UGTPg1* gene because UGT109A1 can transfer a glucose moiety to not only C3−OH but also C20−OH of DM[6]. The above four strains and YDP were cultivated in YPD medium for 3 days in triplicate to compare their titers of 3*β*,20*S*-Di-*O*-Glc-DM. The strain YDS with the highest titer of 3*β*,20*S*-Di-*O*-Glc-DM was retained for further engineering.

The integration module containing the upstream pathway genes *IDI1*, *ERG20*, *ERG9*, *ERG1*, antisense *ERG7* and *LEU* (Supporting Information Fig. S3) was transformed into the *δ*4 site of YF2-C and YDS, resulting in the strains YFC1 and YS1, respectively. The integration module containing the aforementioned genes and the transcriptional activator gene *HAC1* (Fig. S3) was transformed into the *δ*4 site of YF2-C and YDS, resulting in the strains YFC2 and YS2, respectively. The integration module containing the aforementioned genes and the transcriptional activator gene *INO2* (Fig. S3) was transformed into the *δ*4 site of YF2-C and YDS, resulting in the strains YFC3 and YS3, respectively. The integration module containing the aforementioned genes and the transcriptional activator genes *HAC1* and *INO2* (Fig. S3) was transformed into the *δ*4 site of YF2-C and YDS, resulting in the strains YFC4 and YS4, respectively. A total of 10 single colonies were randomly picked from SD-HIS-URA-LEU plates, respectively, and cultivated in YPD medium for 3 days to compare the titers of their respective target products. The strains YFC2 and YS3 with the highest titers of their respective target products were used for further engineering.

The integration module containing the gene expression cassettes of *PGM1*, *PGM2*, *UGP1* together with *TRP* (Supporting Information Fig. S4) was transformed into the *rDNA* site of YFC2 and YS3, resulting in the strains YFR and YSR. Similarly, the same integration module was transformed into the *EGH1* site of YFC2 and YS3, resulting in the strains YFE and YSE. A total of 10 single colonies were selected randomly from SD-HIS-URA-LEU-TRP plates, respectively, and cultivated in YPD medium for 3 days to compare the titers of their respective target products.

The strains constructed in this study are listed in Table 1.

2.5. Yeast cultivation and fed-batch fermentation

The strains were first inoculated into 10 mL SD medium and grown at 30 °C and 220 rpm for 18 h, and then transferred to 150 mL YPD medium in 500 mL shake flask with an initial OD_{600} of 0.2 and grown at 30 °C and 220 rpm for 6 days. 5 mL fed solution described previously[24] was fed into the medium at 48, 72, 96 and 120 h, respectively.

Fed-batch fermentation of the strain YSR was conducted as described previously[24]. About 100 mL seed cultures were inoculated into 1 L YPD medium in a 3 L bioreactor. Fermentation was carried out at 30 °C. The pH was controlled at 5.5 by addition of ammonium hydroxide. Dissolved O_2 was controlled at approximately 30% by the agitation cascade and air flow rate.

2.6. Metabolite extraction

Ginsenosides F2, 3*β*,20*S*-Di-*O*-Glc-DM, 3*β*-*O*-Glc-DM, 20*S*-*O*-Glc-DM, compound K and Rh2 were extracted from the cell pellets and the supernatant with *n*-butanol, while aglycones DM and PPD were extracted with *n*-hexane.

2.7. HPLC, LC−MS and NMR analysis

All the chemicals were analyzed by HPLC (Agilent 1260 Infinity II). Chromatographic separation was performed at 28 °C with a Cosmosil 5C18-MS-II column (5 μm, 4.6 mm × 150 mm). The flow rate was 1 mL/min and the detecting wavelength was 203 nm. The mobile phase consisted of water and acetonitrile (ACN). The separation of ginsenosides (F2, 3*β*,20*S*-Di-*O*-Glc-DM, 3*β*-*O*-Glc-DM, 20*S*-*O*-Glc-DM, compound K and Rh2) was conducted using gradient procedure as follow: 0−20 min (20%−85% ACN), 20−30 min (85%−100% ACN), 30−40 min (100% ACN), 40−45 min (20% ACN). The separation of ginsenoside aglycones (DM and PPD) was conducted using the isocratic procedure as follow: 0−30 min (85% ACN). Semi-preparative HPLC and LC−MS were performed as described previously[22]. NMR spectra were recorded on an INOVA 500 NMR spectrometer (Varian, CA, USA) in CD_3OD with TMS as an internal standard.

2.8. In vivo evaluation of the anti-pancreatic cancer activities of F2 and 3β,20S-Di-O-Glc-DM

C57BL/6J mice (14−18 g, male) were purchased from NIFDC (Beijing, China). PAN02 tumors inoculated in the axillae of mice were stripped under aseptic conditions and made into the tissue cell suspension. Then the cells were diluted to 2×10^7 cells/mL. 0.2 mL cell suspension was subcutaneously implanted in the left flank of each mouse. The mice were randomly divided into eight groups after being inoculated for 24 h. Model control was administered with 30% PEG400, positive control was administered with 10.0 mg/kg Rg3, and the other six groups were continuously administered with 5.0 mg/kg, 10.0 mg/kg and 20.0 mg/kg of F2 or 3*β*,20*S*-Di-*O*-Glc-DM (dissolved in 30% PEG400) for 11 days, once a day (i.g.). The tumors were excised and weighed to calculate the inhibition rate (IR) of tumor growth after the mice were euthanized.

3. Results and discussion

3.1. Production of ginsenosides F2 and 3β,20S-Di-O-Glc-DM by enzymatic catalysis with PgUGT74AE2 and UGTPg1

In previous studies, it was demonstrated that PgUGT74AE2 from *P. ginseng* could transfer a glucose moiety to C3-OH of PPD and DM to produce ginsenosides Rh2 and 3*β*-*O*-Glc-DM, respectively, while UGTPg1 from *P. ginseng* could transfer a glucose moiety to

Table 1 Strains constructed in this study.

Strain	Description
YF2	P_{TEF1}-*DS-GFP*-T_{CYC1}, P_{PGK1}-*tHMG1*-T_{ADH1}, P_{PYK1}-*PPDS*-T_{ADH2}, P_{TDH3}-*ATR2*-T_{TPI1}, P_{TEF1}-*UGTPg1*-T_{ADH2}, P_{PGK1}-*UGT74AE2*-T_{CYC1} and *HIS* marker gene were integrated into the δ1 site of Y-ΔHXK2 with p-Cas9-gRNA
YF2-B	P_{TEF1}-*DS-GFP*-T_{CYC1}, P_{PGK1}-*tHMG1*-T_{ADH1}, P_{TDH3}-*PPDS*-T_{ADH2}, P_{PYK1}-*ATR2*-T_{TPI1}, P_{TEF1}-*UGTPg1*-T_{ADH2}, P_{PGK1}-*UGT74AE2*-T_{CYC1} and *HIS* marker gene were integrated into the δ1 site of Y-ΔHXK2 with p-Cas9-gRNA
YF2-C	P_{TEF1}-*DS-GFP*-T_{CYC1}, P_{PGK1}-*tHMG1*-T_{ADH1}, P_{TDH3}-*PPDS*-T_{ADH2}, P_{TEF2}-*ATR2*-T_{TPI1}, P_{TEF1}-*UGTPg1*-T_{ADH2}, P_{PGK1}-*UGT74AE2*-T_{CYC1} and *HIS* marker gene were integrated into the δ1 site of Y-ΔHXK2 with p-Cas9-gRNA
YDP	P_{TEF1}-*DS-GFP*-T_{CYC1}, P_{PGK1}-*tHMG1*-T_{ADH1}, P_{TDH3}-*UGTPg1*-T_{ADH2}, P_{TEF1}-*UGT74AE2*-T_{CYC1} and *HIS* marker gene were integrated into the δ1 site of Y-ΔHXK2 with p-Cas9-gRNA
YDS	P_{TEF1}-*DS-GFP*-T_{CYC1}, P_{PGK1}-*tHMG1*-T_{ADH1}, P_{TDH3}-*UGTPg1*-T_{ADH2}, P_{TEF1}-*M7*-T_{CYC1} and *HIS* marker gene were integrated into the δ1 site of Y-ΔHXK2 with p-Cas9-gRNA
YDN	P_{TEF1}-*DS-GFP*-T_{CYC1}, P_{PGK1}-*tHMG1*-T_{ADH1}, P_{TDH3}-*UGTPg1*-T_{ADH2}, P_{TEF1}-*UGTPn50-HV*-T_{CYC1} and *HIS* marker gene were integrated into the δ1 site of Y-ΔHXK2 with p-Cas9-gRNA
YDC	P_{TEF1}-*DS-GFP*-T_{CYC1}, P_{PGK1}-*tHMG1*-T_{ADH1}, P_{TDH3}-*UGTPg1*-T_{ADH2}, P_{TEF1}-*M7-1*-T_{CYC1} and *HIS* marker gene were integrated into the δ1 site of Y-ΔHXK2 with p-Cas9-gRNA
YDB	P_{TEF1}-*DS-GFP*-T_{CYC1}, P_{PGK1}-*tHMG1*-T_{ADH1}, P_{TDH3}-*UGT109A1*-T_{ADH2} and *HIS* marker gene were integrated into the δ1 site of Y-ΔHXK2 with p-Cas9-gRNA
YFC1	P_{TDH3}-*IDI1*-T_{TPI1}, P_{PGK1}-*ERG20*-T_{ADH1}, P_{TEF1}-*ERG9*-T_{CYC1}, P_{PGK1}-*ERG1*-T_{ADH1}, P_{TEF1}-*ERG7*-T_{CYC1} and *LEU* marker gene were integrated into the δ4 site of YF2-C
YFC2	P_{TDH3}-*IDI1*-T_{TPI1}, P_{PGK1}-*ERG20*-T_{ADH1}, P_{TEF1}-*ERG9*-T_{CYC1}, P_{PGK1}-*ERG1*-T_{ADH1}, P_{TEF1}-*ERG7*-T_{IDP1}, P_{ENO2}-*HAC1*-T_{FBA1} and *LEU* marker gene were integrated into the δ4 site of YF2-C
YFC3	P_{TDH3}-*IDI1*-T_{TPI1}, P_{PGK1}-*ERG20*-T_{ADH1}, P_{TEF1}-*ERG9*-T_{CYC1}, P_{PGK1}-*ERG1*-T_{ADH1}, P_{TEF1}-*ERG7*-T_{IDP1}, P_{TEF2}-*INO2*-T_{TDH2} and *LEU* marker gene were integrated into the δ4 site of YF2-C
YFC4	P_{TDH3}-*IDI1*-T_{TPI1}, P_{PGK1}-*ERG20*-T_{ADH1}, P_{TEF1}-*ERG9*-T_{CYC1}, P_{PGK1}-*ERG1*-T_{ADH1}, P_{TEF1}-*ERG7*-T_{IDP1}, P_{ENO2}-*HAC1*-T_{FBA1}, P_{TEF2}-*INO2*-T_{TDH2} and *LEU* marker gene were integrated into the δ4 site of YF2-C
YS1	P_{TDH3}-*IDI1*-T_{TPI1}, P_{PGK1}-*ERG20*-T_{ADH1}, P_{TEF1}-*ERG9*-T_{CYC1}, P_{PGK1}-*ERG1*-T_{ADH1}, P_{TEF1}-*ERG7*-T_{CYC1} and *LEU* marker gene were integrated into the δ4 site of YDS
YS2	P_{TDH3}-*IDI1*-T_{TPI1}, P_{PGK1}-*ERG20*-T_{ADH1}, P_{TEF1}-*ERG9*-T_{CYC1}, P_{PGK1}-*ERG1*-T_{ADH1}, P_{TEF1}-*ERG7*-T_{IDP1}, P_{ENO2}-*HAC1*-T_{FBA1} and *LEU* marker gene were integrated into the δ4 site of YDS
YS3	P_{TDH3}-*IDI1*-T_{TPI1}, P_{PGK1}-*ERG20*-T_{ADH1}, P_{TEF1}-*ERG9*-T_{CYC1}, P_{PGK1}-*ERG1*-T_{ADH1}, P_{TEF1}-*ERG7*-T_{IDP1}, P_{TEF2}-*INO2*-T_{TDH2} and *LEU* marker gene were integrated into the δ4 site of YDS
YS4	P_{TDH3}-*IDI1*-T_{TPI1}, P_{PGK1}-*ERG20*-T_{ADH1}, P_{TEF1}-*ERG9*-T_{CYC1}, P_{PGK1}-*ERG1*-T_{ADH1}, P_{TEF1}-*ERG7*-T_{IDP1}, P_{ENO2}-*HAC1*-T_{FBA1}, P_{TEF2}-*INO2*-T_{TDH2} and *LEU* marker gene were integrated into the δ4 site of YDS
YFR	P_{TEF1}-*PGM1*-T_{CYC1}, P_{PGK1}-*PGM2*-T_{ADH1}, P_{TDH3}-*UGP1*-T_{ADH2} and *TRP* marker gene were integrated into the *rDNA* site of YFC2
YFE	P_{TEF1}-*PGM1*-T_{CYC1}, P_{PGK1}-*PGM2*-T_{ADH1}, P_{TDH3}-*UGP1*-T_{ADH2} and *TRP* marker gene were integrated into the *EGH1* site of YFC2
YSR	P_{TEF1}-*PGM1*-T_{CYC1}, P_{PGK1}-*PGM2*-T_{ADH1}, P_{TDH3}-*UGP1*-T_{ADH2} and *TRP* marker gene were integrated into the *rDNA* site of YS3
YSE	P_{TEF1}-*PGM1*-T_{CYC1}, P_{PGK1}-*PGM2*-T_{ADH1}, P_{TDH3}-*UGP1*-T_{ADH2} and *TRP* marker gene were integrated into the *EGH1* site of YS3

C20−OH of PPD and DM to produce compound K and 20*S*-*O*-Glc-DM, respectively[24,27]. However, it has not been reported so far that PgUGT74AE2 and UGTPg1 can transfer a glucose moiety to C3−OH and C20−OH of PPD and DM simultaneously to produce F2 and 3β,20*S*-Di-*O*-Glc-DM, respectively. In order to demonstrate this, recombinant PgUGT74AE2 and UGTPg1 were incubated simultaneously with UDPG as the glycosyl donor, PPD and DM as the glycosyl acceptors, respectively. The production of F2 and 3β,20*S*-Di-*O*-Glc-DM was confirmed by LC−MS, ^{1}H and ^{13}C NMR (Fig. 1, Supporting Information Figs. S5 and S6). The results indicated that both F2 and 3β,20*S*-Di-*O*-Glc-DM could be produced by *in vitro* enzymatic catalysis with PgUGT74AE2 and UGTPg1, which also meant that PgUGT74AE2 and UGTPg1 could be used as basic functional elements to construct the metabolic pathways of F2 and 3β,20*S*-Di-*O*-Glc-DM in microbes. *In vitro* enzymatic catalysis for the production of F2 and 3β,20*S*-Di-*O*-Glc-DM requires expensive UDPG as the glycosyl donor, PPD and DM as the glycosyl receptors, thereby limiting its practical application. Therefore, we aimed to construct the yeast cell factories for the *de novo* production of F2 and 3β,20*S*-Di-*O*-Glc-DM from cheap glucose.

3.2. *Constructing yeast cell factories for the de novo biosynthesis of ginsenosides F2 and 3β,20S-Di-O-Glc-DM*

Besides enzymatic catalysis, metabolic engineering of *S. cerevisiae* has been widely used as a green and sustainable biotechnology to produce natural and unnatural products[24]. It was reported that deletion of *HXK2* gene could promote the biosynthesis of exogenous terpenoids in *S. cerevisiae* probably because metabolic flux change in the mutant led to reinforcement of the glycolysis flux to the MVA pathway[28]. Previously, we knocked out

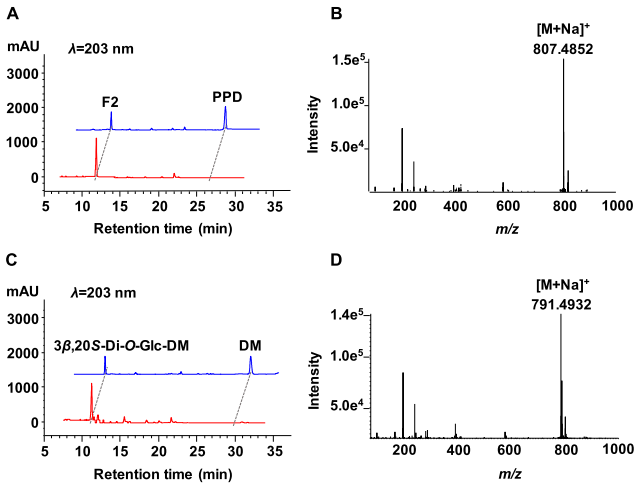

Figure 1 Identification of the products by *in vitro* enzymatic catalysis. (A) HPLC analysis of the product of PPD catalyzed by PgUGT74AE2 and UGTPg1. Blue, authentic samples; red, the product of enzymatic catalysis. (B) The MS spectrum of the product of PPD catalyzed by PgUGT74AE2 and UGTPg1. (C) HPLC analysis of the product of DM catalyzed by PgUGT74AE2 and UGTPg1. Blue, authentic samples; red, the product of enzymatic catalysis. (D) The MS spectrum of the product of DM catalyzed by PgUGT74AE2 and UGTPg1.

HXK2 gene to boost the production of ginsenosides in *S. cerevisiae*, resulting in the optimized chassis strain Y-ΔHXK2[24]. To construct the biosynthetic pathway of F2 in *S. cerevisiae*, the gene expression module containing *DS*, *PPDS*, *PgUGT74AE2*, *UGTPg1* from *P. ginseng*, *ATR2* from *A. thaliana* and *tHMG1* from *S. cerevisiae* was integrated into the δ1 site of Y-ΔHXK2 *via* the CRISPR/Cas9 system (Fig. 2 and Fig. S1). Likewise, the biosynthetic pathway of 3β,20*S*-Di-*O*-Glc-DM was constructed by introducing the gene expression module containing *DS*, *UGTPg1*, *PgUGT74AE2* and *tHMG1* into the δ1 site of Y-ΔHXK2 (Fig. 2 and Fig. S2). A total of 10 transformants from each group were randomly picked and cultivated to identify the products and compare their titers. As expected, LC−MS analysis of intracellular and extracellular extracts confirmed the production of F2 (Fig. 3A and B) or 3β,20*S*-Di-*O*-Glc-DM (Fig. 3C and D) in these transformants. The transformants with the highest titers of F2 and 3β,20*S*-Di-*O*-Glc-DM were named as YF2 and YDP, respectively (Fig. 4). F2 and 3β,20*S*-Di-*O*-Glc-DM were isolated from YF2 and YDP, respectively, purified by semi-preparative HPLC, and identified by comparing their ^{1}H and ^{13}C NMR spectroscopic data with F2 and 3β,20*S*-Di-*O*-Glc-DM produced by the above enzymatic catalysis.

3.3. *Tuning the promoters of PPDS and ATR2 genes to increase the production of ginsenoside F2*

The balance between CYP450 enzymes and their reductases has a great effect on the biosynthesis of natural products[29,30]. To boost the production of F2, we tuned the promoters of *PPDS* and *ATR2* genes. In the strain YF2, the promoters of *PPDS* and *ATR2* genes were the weak promoter *PYK1* and the strong promoter *TDH3*, respectively. The strain YF2-B was constructed with *PPDS* gene under the strong promoter *TDH3* and *ATR2* gene under the weak promoter *PYK1*, while the strain YF2-C was constructed with *PPDS* and *ATR2* genes under the strong promoters *TDH3* and *TEF2*, respectively. As shown in Table 2, after being cultivated for 6 days, the highest titer of F2 reached 8.8 mg/L in YF2-C, which was 7.3-fold higher than that of YF2 (1.2 mg/L). Meanwhile, the titer of intermediate Rh2 in YF2-C (2.4 mg/L) was 8.0-fold higher than that of YF2 (0.3 mg/L). In addition, the titer of PPD in YF2-C (51.0 mg/L) was also higher than that of YF2 (37.7 mg/L). These results indicated that the simultaneous utilization of the strong promoters for the expression of *PPDS* and *ATR2* genes could significantly improve the production of F2. The reason for this was probably that the overexpression of *PPDS* and *ATR2* genes could promote the conversion from DM to PPD, which was the bottleneck of F2 biosynthesis.

3.4. *Using the high-efficiency C3-glycosyltransferase to increase the production of 3β,20S-Di-O-Glc-DM*

To improve the production of 3β,20*S*-Di-*O*-Glc-DM, we screened the genes of high-efficiency C3-glycosyltransferases from different species, including M7 (mutant of UGT74AC1) from *S. grosvenorii*[25], UGTPn50-HV (mutant of UGTPn50) from *P. notoginseng*[22], M7-1 (mutant of UGT51) from *S. cerevisiae*[26] and UGT109A1 from *B. subtilis*[6]. The biosynthetic pathway of 3β,20*S*-Di-*O*-Glc-DM was constructed in Y-ΔHXK2 by replacing the *PgUGT74AE2* gene with the codon-optimized *M7*, *UGTPn50-HV*, *M7-1* and *UGT109A1* genes, resulting in the strains YDS, YDN, YDC and YDB, respectively. After being cultivated for 3 days, the titers of 3β,20*S*-Di-*O*-Glc-DM in both YDC and YDB strains were found to be much lower than that of YDP, and YDS had the highest titer of 3β,20*S*-Di-*O*-Glc-DM among the above five strains (Fig. 4). It suggested that C3-glycotransferases from plants were more efficient for the production of 3β,20*S*-Di-*O*-Glc-DM in the engineered yeasts than those from microbes. After being cultivated for 6 days, the titer of 3β,20*S*-Di-*O*-Glc-DM in YDS reached 90.5 mg/L, 1.1-fold higher than that of YDP (82.0 mg/L) (Table 2). Besides, the titer of the intermediate 3β-*O*-Glc-DM in YDS (3.5 mg/L) was higher than that of YDP (2.2 mg/L), whereas the titer of the intermediate 20*S*-*O*-Glc-DM in YDS (0.3 mg/L) was much lower than that of YDP (1.6 mg/L). We speculated that the high efficiency of C3-glycosyltransferase M7 led to more DM towards 3β-*O*-Glc-DM.

3.5. *Improving the precursor supply and overexpressing the transcriptional activators to increase the production of ginsenosides F2 and 3β,20S-Di-O-Glc-DM*

Previous studies have shown that the improved precursor supply is conducive to increasing the production of the target products in the engineered yeasts[22,31−33]. Therefore, we have employed the strategies of overexpressing the key enzymes involved in the upstream biosynthetic pathway and tuning down the competitive ergosterol biosynthetic pathway to enhance the yields of ginsenosides in the engineered yeasts[6,24]. To increase the production of F2 and 3β,20*S*-Di-*O*-Glc-DM, we constructed the expression module containing the expression cassettes of *IDI1*, *ERG20*, *ERG9*, *ERG1* and antisense *ERG7* genes, and integrated it into the δ4 site of the F2-producing strain YF2-C and the 3β,20*S*-Di-*O*-Glc-DM-producing strain YDS, resulting in the strains YFC1 and YS1, respectively. After being cultivated for 3 days, the titers of F2 in YFC1 and 3β,20*S*-Di-*O*-Glc-DM in YS1 were 1.1- and 1.6-fold higher than those of YF2-C and YDS, respectively (Fig. 4). Optimizing the upstream biosynthetic pathway improved the

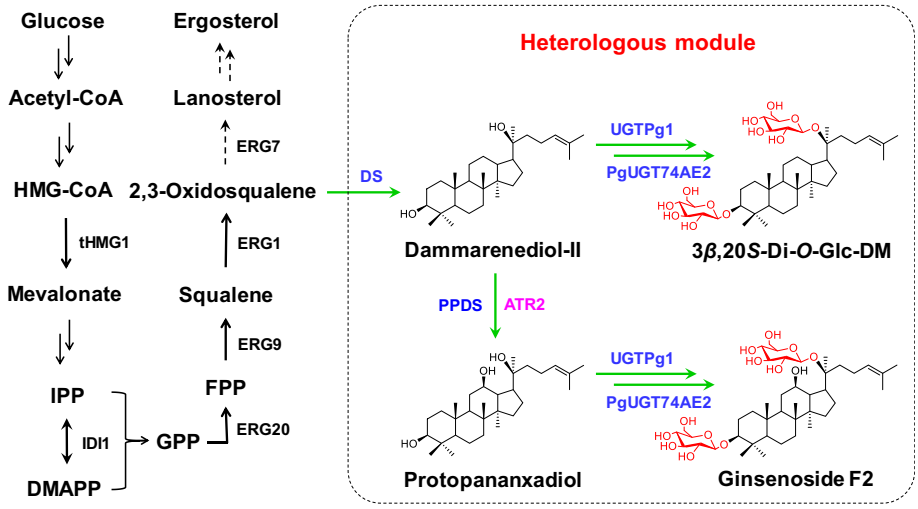

Figure 2 The biosynthetic pathways of ginsenosides F2 and 3*β*,20*S*-Di-*O*-Glc-DM in the engineered yeasts.

production of 3*β*,20*S*-Di-*O*-Glc-DM but did not apparently improve the production of F2, suggesting that the conversion from DM to PPD was a rate-limiting step in F2 biosynthesis.

The expression levels of the heterologous enzymes in *S. cerevisiae* significantly affect the production of the target products. The transcriptional activator HAC1 is a major regulator of the unfolded protein response in many eukaryotes, which can up-regulate the expression of the heterologous enzymes[34]. We previously showed that the titers of the unnatural ginsenosides 3*β*-*O*-Glc-DM and 20*S*-*O*-Glc-DM in the engineered yeasts were increased by 1.6- and 1.5-fold, respectively, by overexpressing HAC1[24]. INO2 is a key endoplasmic reticulum (ER) size regulator, which can enlarge ER. By overexpressing INO2, the production of squalene and PPD in the engineered yeasts were increased by 71- and 8-fold, respectively[35]. In view of this, the expression module containing *IDI1*, *ERG20*, *ERG9*, *ERG1*, antisense *ERG7* genes together with the transcriptional activator *HAC1* and/or *INO2* genes, was transformed into the strains YF2-C and YDS, respectively, resulting in the strains YFC2, YFC3, YFC4, YS2, YS3 and YS4 correspondingly (Table 1). As a result, in F2-producing yeasts, up-regulating the upstream pathway and simultaneously overexpressing HAC1 could maximize the production of F2 (Fig. 4). After being cultivated for 6 days, the titer of F2 in YFC2 reached 16.8 mg/L, which was 1.9-fold higher than that of YF2-C (8.8 mg/L, Table 2). In 3*β*,20*S*-Di-*O*-Glc-DM-producing yeasts, up-regulating the upstream pathway and simultaneously overexpressing INO2 could maximize the production of 3*β*,20*S*-Di-*O*-Glc-DM (Fig. 4). The titer of 3*β*,20*S*-Di-*O*-Glc-DM in YS3 reached 175.1 mg/L, which was 1.9-fold higher than that of YDS (90.5 mg/L, Table 2). These results demonstrated that improving the precursor supply together with overexpressing transcriptional activators led to the increased production of F2 and 3*β*,20*S*-Di-*O*-Glc-DM. Moreover, overexpressing HAC1 was more effective for the production of F2, while overexpressing INO2 was more effective for the production of 3*β*,20*S*-Di-*O*-Glc-DM.

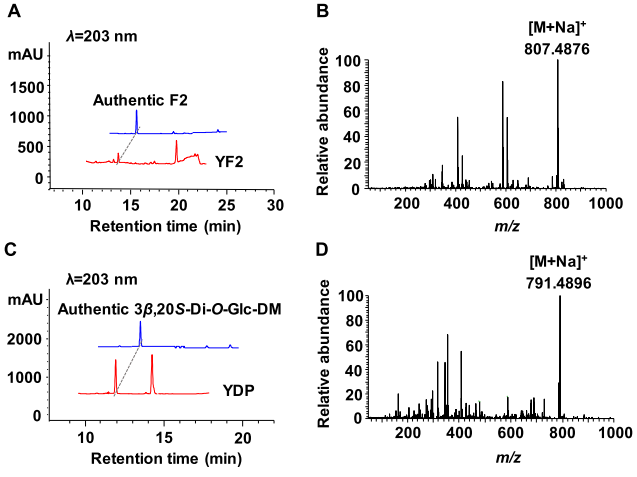

Figure 3 Identification of the fermentation products of the engineered yeasts. (A) HPLC analysis of the product of the strain YF2. (B) The MS spectrum of the product of the strain YF2. (C) HPLC analysis of the product of the strain YDP. (D) The MS spectrum of the product of the strain YDP.

3.6. Improving the UDPG supply to increase the production of ginsenosides F2 and 3β,20S-Di-O-Glc-DM

In the previous section, we increased the titers of F2 and 3*β*,20*S*-Di-*O*-Glc-DM by improving the supply of the ginsenoside aglycones (glycosyl receptors). Meanwhile, the supply of the glycosyl donors is also important for the production of ginsenosides. It was reported that enhancing the supply of UDPG significantly improved the yields of ginsenoside Rh2 and compound K in the engineered yeasts[26,36]. PGM1, PGM2 and UGP1 are the key enzymes involved in the UDPG biosynthesis. In our present study, we overexpressed the three enzymes for higher titers of F2 and 3*β*,20*S*-Di-*O*-Glc-DM. We constructed the expression cassettes of *PGM1*, *PGM2* and *UGP1* genes under the strong promoters of *TEF1*, *PGK1* and *TDH3*, respectively, to maximize the expression levels of these enzymes. Then we integrated them into the multi-copy *rDNA* site of the strains YFC2 and YS3, respectively, resulting in the strains YFR and YSR. In addition, EGH1 in *S. cerevisiae* is a glucosidase with broad specificity[37], which can remove the C3-glycosyl of Rh2[26]. Because of the structural

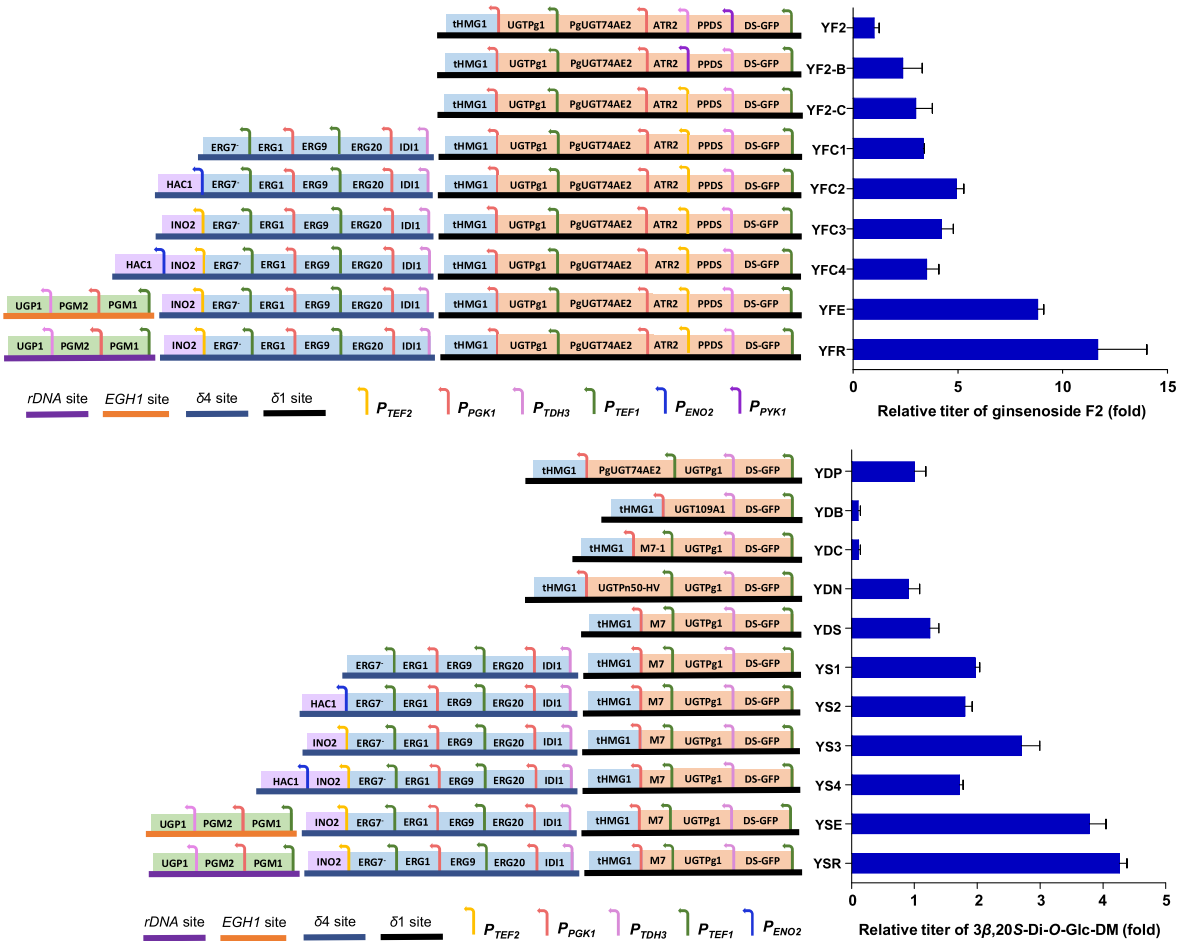

Figure 4 Increasing the production of ginsenosides F2 and 3*β*,20*S*-Di-*O*-Glc-DM in the engineered yeasts by multistep metabolic engineering strategies. The strains were cultivated in YPD medium in shake flasks for 3 days. The genes in blue boxes are involved in the upstream biosynthetic pathway. The genes in orange boxes are involved in the downstream biosynthetic pathway. The genes in green boxes are involved in the UDPG biosynthetic pathway. The genes in purple boxes are the transcriptional activator genes.

Table 2 The production of ginsenosides F2, 3*β*,20*S*-Di-*O*-Glc-DM and their intermediates in the engineered yeasts by fed-batch fermentation in shake flasks for 6 days.

Strain	Biomass (g/L)	F2 (mg/L)	Rh2 (mg/L)	Compound K (mg/L)	3*β*,20*S*-*O*-Glc-DM (mg/L)	3*β*-*O*-Glc-DM (mg/L)	20*S*-*O*-Glc-DM (mg/L)	PPD (mg/L)	DM (mg/L)
YF2	13.9	1.2	0.3	0.0	0.8	0.7	0.6	37.7	14.5
YF2-C	13.7	8.8	2.4	0.0	3.0	0.6	0.2	51.0	31.4
YFC2	16.3	16.8	2.3	0.0	5.8	0.7	0.1	50.2	29.1
YFR	14.8	21.0	4.3	0.0	18.1	0.2	0.0	31.1	33.8
YDP	12.9	–	–	–	82.0	2.2	1.6	–	21.6
YDS	14.6	–	–	–	90.5	3.5	0.3	–	23.3
YS3	14.2	–	–	–	175.1	10.5	1.9	–	69.3
YSR	15.0	–	–	–	346.1	14.2	2.1	–	49.2

The MS spectra of the intermediates (Rh2, compound K, 3*β*-*O*-Glc-DM, 20*S*-*O*-Glc-DM, PPD and DM) are listed in Supporting Information Fig. S7. –Not applicable.

similarity among F2, 3*β*,20*S*-Di-*O*-Glc-DM and Rh2, we speculated that EGH1 might also hydrolyze F2 and 3*β*,20*S*-Di-*O*-Glc-DM. Therefore, the expression module containing *PGM1*, *PGM2* and *UGP1* was integrated into the *EGH1* site of YFC2 and YS3 to overexpress the UDPG biosynthetic genes and knock out *EGH1* simultaneously, resulting in the strains YFE and YSE. The titer of F2 in YFR was higher than that of YFE (Fig. 4) and reached 21.0 mg/L after being cultivated for 6 days, which was 1.3-fold higher than that of YFC2 (16.8 mg/L, Table 2). The titer of 3*β*,20*S*-Di-*O*-Glc-DM in YSR was higher than that of YSE (Fig. 4) and reached 346.1 mg/L after being cultivated for 6 days, which was 2.0-fold higher than that of YS3 (175.1 mg/L, Table 2). Simultaneously, the titer of the precursor PPD of F2 in YFR (31.1 mg/L) was lower than that of YFC2 (50.2 mg/L), and the

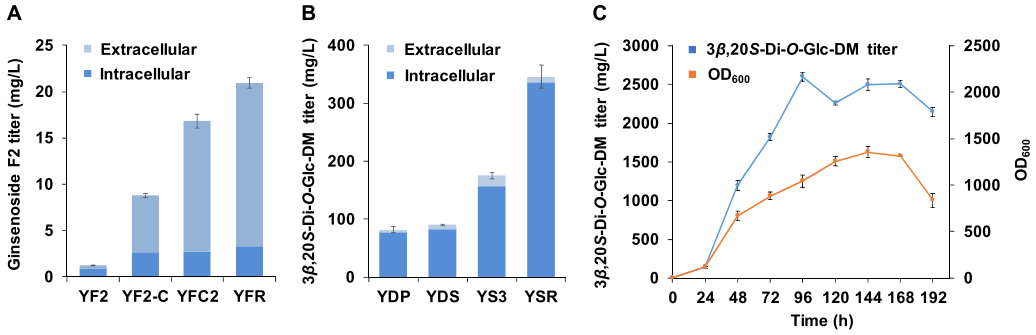

Figure 5 Production of ginsenosides F2 and 3β,20*S*-Di-*O*-Glc-DM in the engineered yeasts. (A) Production of F2 in shake flasks. The strains were cultivated in YPD medium by fed-batch fermentation for 6 days. (B) Production of 3β,20*S*-Di-*O*-Glc-DM in shake flasks. The strains were cultivated in YPD medium by fed-batch fermentation for 6 days. (C) Production of 3β,20*S*-Di-*O*-Glc-DM in YSR by fed-batch fermentation in a 3 L bioreactor.

titer of the precursor DM of 3β,20*S*-Di-*O*-Glc-DM in YSR (49.2 mg/L) was also lower than that of YS3 (69.3 mg/L, Table 2). These results demonstrated that in both F2-producing and 3β,20*S*-Di-*O*-Glc-DM-producing yeasts, multi-copy integration of the UDPG biosynthetic genes was more effective for the high production of target products than single-copy integration of them together with deletion of *EGH1* gene. Furthermore, the titers of the precursor PPD of F2 in YFR and the precursor DM of 3β,20*S*-Di-*O*-Glc-DM in YSR were both lower than those of their respective controls, indicating that increasing UDPG supply could improve the conversion from precursors to target products.

Taken together, we were able to increase the titers of F2 and 3β,20*S*-Di-*O*-Glc-DM in the engineered yeasts by 17.5-fold (from 1.2 to 21.0 mg/L) and 4.2-fold (from 82.0 to 346.1 mg/L), respectively, by multistep metabolic engineering strategies (Table 2, Fig. 5A and B). However, the titer of F2 was much lower than that of 3β,20*S*-Di-*O*-Glc-DM probably because the biosynthesis of F2 has one more rate-limiting step from DM to PPD than that of 3β,20*S*-Di-*O*-Glc-DM. Surprisingly, F2 was mainly detected extracellularly, but 3β,20*S*-Di-*O*-Glc-DM was mainly detected intracellularly. The reason for this phenomenon needs to be further investigated. Moreover, little compound K was detected in F2-producing strains. It seems likely that compound K produced in F2-producing cells could be rapidly converted to F2. Lots of aglycones PPD and DM still accumulated in the engineered strains, probably due to the low catalytic efficiency of the UDP-glycosyltransferases. Therefore, to increase both the catalytic efficiency of UDP-glycosyltransferases by protein engineering and their gene copy numbers in the engineered yeasts is expected to further boost the titers of F2 and 3β,20*S*-Di-*O*-Glc-DM in the future. In addition, during the optimization process of the engineered yeasts, the cell biomass after fermentation did not decrease, but rather increased slightly, suggesting that the enhanced production of F2 and 3β,20*S*-Di-*O*-Glc-DM did not interfere with cell growth of the engineered yeasts (Table 2).

3.7. *Evaluating the anti-pancreatic cancer activity of ginsenosides F2 and 3β,20S-Di-O-Glc-DM*

Several previous studies reported that F2 exhibited anti-glioma[3], anti-breast cancer[4] and anti-gastric cancer[5] activities. However, the anti-pancreatic cancer activity of F2 and 3β,20*S*-Di-*O*-Glc-DM has never been reported before. Accordingly, we evaluated them in the PAN02 model. Rg3 was used as the positive control because it has been developed to be an anti-tumor drug (Shenyi capsules) for twenty years and has a good performance in the clinic application. The results are shown in Table 3. In the group treated with 10 mg/kg F2, the inhibition rate was 42.9%, which was slightly lower than that of 10 mg/kg Rg3 (44.5%). In the group treated with 5 mg/kg 3β,20*S*-Di-*O*-Glc-DM, the inhibition rate was 47.0%, which was higher than that of 10 mg/kg Rg3. The results demonstrated that both F2 and 3β,20*S*-Di-*O*-Glc-DM have anti-pancreatic cancer activity. Especially, it was inspiring that 3β,20*S*-Di-*O*-Glc-DM displayed better activity even at a lower concentration than both Rg3 and F2.

Table 3 *In vivo* evaluation of anti-tumor activity of ginsenosides F2 and 3β,20*S*-Di-*O*-Glc-DM in the PAN02 model.

Group	Dosage	Body weight (g)		Tumor weight	Inhibition rate
	(mg/kg)	Begin	End	(g)	(%)
Negative control	–	18.1 ± 0.5	20.7 ± 1.1	2.45 ± 0.54	–
Rg3	10.0	17.4 ± 0.4	20.5 ± 1.1	1.36 ± 0.57**	44.5
F2	5.0	17.5 ± 0.7	21.0 ± 0.9	1.60 ± 0.55*	34.7
	10.0	17.3 ± 0.3	20.7 ± 1.2	1.40 ± 0.33***	42.9
	20.0	16.9 ± 0.7	20.4 ± 2.2	2.03 ± 0.55	17.0
3β,20*S*-Di-*O*-Glc-DM	5.0	17.6 ± 0.5	21.0 ± 0.9	1.30 ± 0.23***	47.0
	10.0	17.7 ± 0.8	20.3 ± 1.9	1.74 ± 0.58*	29.0
	20.0	17.2 ± 0.5	20.8 ± 1.2	1.60 ± 0.71*	34.6

*$P < 0.05$, **$P < 0.01$ and ***$P < 0.001$, compared with the vehicle control. –Not applicable.

3.8. *Conducting fed-batch fermentation to increase the production of 3β,20S-Di-O-Glc-DM*

Fed-batch fermentation can significantly improve the cell density, and then improve the production of target products, which has been used to produce artemisinin acid[10], miltiradiene[11], resveratrol[38] and ginsenosides[39]. After optimizing the engineered yeasts at the gene level, we achieved notable increase in the production of F2 and 3*β*,20*S*-Di-*O*-Glc-DM. Considering the higher production and the better pharmacological activity of 3*β*,20*S*-Di-*O*-Glc-DM than F2, we chose the engineered strain YSR for fed-batch fermentation in a 3 L bioreactor to further improve the titer of 3*β*,20*S*-Di-*O*-Glc-DM. The cell biomass continued to increase at the early stage of the fermentation and reached the maximum OD_{600} of 1356 at 144 h (Fig. 5C). The production of 3*β*,20*S*-Di-*O*-Glc-DM continued to increase until the highest titer reached 2.6 g/L at 96 h. After that, the titer of 3*β*,20*S*-Di-*O*-Glc-DM began to decrease slightly. At the end of the fermentation, the titer of 3*β*,20*S*-Di-*O*-Glc-DM was 2.1 g/L at 192 h (Fig. 5C). Ultimately, the titer of 3*β*,20*S*-Di-*O*-Glc-DM was remarkably increased by 7.5-fold (from 346.1 mg/L to 2.6 g/L) by fed-batch fermentation. The result provides a favorable condition for industrial production of 3*β*,20*S*-Di-*O*-Glc-DM.

4. Conclusions

In this study, we first identified that PgUGT74AE2 and UGTPg1 from *P. ginseng* could catalyze the glycosylation of PPD and DM at C3-OH and C20-OH simultaneously to produce natural ginsenoside F2 and unnatural ginsenoside 3*β*,20*S*-Di-*O*-Glc-DM, respectively. Then we used PgUGT74AE2 and UGTPg1 as basic functional elements to construct the complete biosynthetic pathways of F2 and 3*β*,20*S*-Di-*O*-Glc-DM in *S. cerevisiae*. The titers of F2 and 3*β*,20*S*-Di-*O*-Glc-DM were increased to 21.0 and 346.1 mg/L at shake flask level, respectively, by multistep metabolic engineering strategies. The titer of 3*β*,20*S*-Di-*O*-Glc-DM was much higher than that of F2, and most excitingly, 3*β*,20*S*-Di-*O*-Glc-DM exhibited better anti-pancreatic cancer activity than F2. Hence, we further improved the titer of 3*β*,20*S*-Di-*O*-Glc-DM to 2.6 g/L by fed-batch fermentation in a 3 L bioreactor. As far as we know, this is the first report on demonstrating the anti-pancreatic cancer activity of F2 and 3*β*,20*S*-Di-*O*-Glc-DM, and achieving their *de novo* biosynthesis from glucose in yeast cell factories. Compared with the traditional approaches, the construction of yeast cell factories for producing F2 and 3*β*,20*S*-Di-*O*-Glc-DM can avoid many disadvantages such as low yield and high cost. Therefore, the engineered yeasts constructed in this study can serve as renewable resource for the green and sustainable production of F2 and 3*β*,20*S*-Di-*O*-Glc-DM, which accelerates their industrial application for drug research and development.

Acknowledgments

We thank Prof. Jungui Dai (Institute of Materia Medica, Chinese Academy of Medical Sciences & Peking Union Medical College) for his constructive suggestions on our research work. This research was financially supported by the grants of CAMS Innovation Fund for Medical Sciences (CIFMS) (2021-I2M-1-029, China), the Beijing Natural Science Foundation (7212158, China), the National Natural Science Foundation of China (81673341), PUMC Disciplinary Development of Synthetic Biology (201920100801, China).

Author contributions

Jinling Yang and Ping Zhu designed the experiments; Fenglin Jiang, Chen Zhou, Yan Li and Haidong Deng performed the experiments; Fenglin Jiang, Jinling Yang, Ping Zhu, Ting Gong, Jingjing Chen and Tianjiao Chen analyzed the data; Fenglin Jiang and Jinling Yang wrote the paper; and all authors reviewed the manuscript.

Conflicts of interest

The authors declare no conflicts of interest.

Appendix A. Supporting information

Supporting data to this article can be found online at https://doi.org/10.1016/j.apsb.2022.04.012.

References

1. Lim TG, Lee CC, Dong Z, Lee KW. Ginsenosides and their metabolites: a review of their pharmacological activities in the skin. *Arch Dermatol Res* 2015;**307**:397−403.
2. Murthy HN, Georgiev MI, Kim YS, Jeong CS, Kim SJ, Park SY, et al. Ginsenosides: prospective for sustainable biotechnological production. *Appl Microbiol Biotechnol* 2014;**98**:6243−54.
3. Shin JY, Lee JM, Shin HS, Park SY, Yang JE, Cho SK, et al. Anticancer effect of ginsenoside F2 against glioblastoma multiforme in xenograft model in SD rats. *J Ginseng Res* 2012;**36**:86−92.
4. Mai TT, Moon J, Song Y, Viet PQ, Phuc PV, Lee JM, et al. Ginsenoside F2 induces apoptosis accompanied by protective autophagy in breast cancer stem cells. *Cancer Lett* 2012;**321**:144−53.
5. Mao Q, Zhang PH, Wang Q, Li SL. Ginsenoside F2 induces apoptosis in humor gastric carcinoma cells through reactive oxygen species-mitochondria pathway and modulation of ASK-1/JNK signaling cascade *in vitro* and *in vivo*. *Phytomedicine* 2014;**21**:515−22.
6. Liang HC, Hu ZF, Zhang TT, Gong T, Chen JJ, Zhu P, et al. Production of a bioactive unnatural ginsenoside by metabolically engineered yeasts based on a new UDP-glycosyltransferase from *Bacillus subtilis*. *Metab Eng* 2017;**44**:60−9.
7. Yao H, Vu MD, Liu XW. Recent advances in reagent-controlled stereoselective/stereospecific glycosylation. *Carbohydr Res* 2019;**473**:72−81.
8. He B, Bai X, Tan YM, Xie WT, Feng Y, Yang GY. Glycosyltransferases: mining, engineering and applications in biosynthesis of glycosylated plant natural products. *Synth Syst Biotechnol* 2022;**7**:602−20.
9. Chen RB, Yang S, Zhang L, Zhou YJ. Advanced strategies for production of natural products in yeast. *iScience* 2020;**23**:100879.
10. Paddon CJ, Westfall PJ, Pitera DJ, Benjamin K, Fisher K, McPhee D, et al. High-level semi-synthetic production of the potent antimalarial artemisinin. *Nature* 2013;**496**:528−32.
11. Hu TY, Zhou JW, Tong YR, Su P, Li XL, Liu Y, et al. Engineering chimeric diterpene synthases and isoprenoid biosynthetic pathways enables high-level production of miltiradiene in yeast. *Metab Eng* 2020;**60**:87−96.
12. Ajikumar PK, Xiao WH, Tyo KE, Wang Y, Simeon F, Leonard E, et al. Isoprenoid pathway optimization for Taxol precursor overproduction in *Escherichia coli*. *Science* 2010;**330**:70−4.

13. Galanie S, Thodey K, Trenchard IJ, Filsinger Interrante M, Smolke CD. Complete biosynthesis of opioids in yeast. *Science* 2015;**349**:1095−100.
14. Luo XZ, Reiter MA, d'Espaux L, Wong J, Denby CM, Lechner A, et al. Complete biosynthesis of cannabinoids and their unnatural analogues in yeast. *Nature* 2019;**567**:123−6.
15. Guan RB, Wang MG, Guan ZH, Jin CY, Lin W, Ji XJ, et al. Metabolic engineering for glycyrrhetinic acid production in *Saccharomyces cerevisiae*. *Front Bioeng Biotechnol* 2020;**8**:588255.
16. Brown S, Clastre M, Courdavault V, O'Connor SE. *De novo* production of the plant-derived alkaloid strictosidine in yeast. *Proc Natl Acad Sci U S A* 2015;**112**:3205−10.
17. Liu XN, Cheng J, Zhang GH, Ding WT, Duan LJ, Yang J, et al. Engineering yeast for the production of breviscapine by genomic analysis and synthetic biology approaches. *Nat Commun* 2018;**9**:448.
18. Kim YJ, Zhang D, Yang DC. Biosynthesis and biotechnological production of ginsenosides. *Biotechnol Adv* 2015;**33**:717−35.
19. Yan X, Fan Y, Wei W, Wang PP, Liu QF, Wei YJ, et al. Production of bioactive ginsenoside compound K in metabolically engineered yeast. *Cell Res* 2014;**24**:770−3.
20. Shi YS, Wang D, Li RS, Huang LQ, Dai ZB, Zhang XL. Engineering yeast subcellular compartments for increased production of the lipophilic natural products ginsenosides. *Metab Eng* 2021;**67**:104−11.
21. Wang PP, Wang JL, Zhao GP, Yan X, Zhou ZH. Systematic optimization of the yeast cell factory for sustainable and high efficiency production of bioactive ginsenoside compound K. *Synth Syst Biotechnol* 2021;**6**:69−76.
22. Wang PP, Wei W, Ye W, Li XD, Zhao WF, Yang CS, et al. Synthesizing ginsenoside Rh2 in *Saccharomyces cerevisiae* cell factory at high-efficiency. *Cell Discov* 2019;**5**:5.
23. Li XD, Wang YM, Fan ZJ, Wang Y, Wang PP, Yan X, et al. High-level sustainable production of the characteristic protopanaxatriol-type saponins from *Panax* species in engineered *Saccharomyces cerevisiae*. *Metab Eng* 2021;**66**:87−97.
24. Hu ZF, Gu AD, Liang L, Li Y, Gong T, Chen JJ, et al. Construction and optimization of microbial cell factories for sustainable production of bioactive dammarenediol-II glucosides. *Green Chem* 2019;**21**:3286−99.
25. Li J, Yang JC, Mu SC, Shang N, Liu C, Zhu YM, et al. Efficient *O*-glycosylation of triterpenes enabled by protein engineering of plant glycosyltransferase UGT74AC1. *ACS Catal* 2020;**10**:3629−39.
26. Zhuang Y, Yang GY, Chen XH, Liu Q, Zhang XL, Deng ZX, et al. Biosynthesis of plant-derived ginsenoside Rh2 in yeast *via* repurposing a key promiscuous microbial enzyme. *Metab Eng* 2017;**42**:25−32.
27. Jung SC, Kim W, Park SC, Jeong J, Park MK, Lim S, et al. Two ginseng UDP-glycosyltransferases synthesize ginsenoside Rg3 and Rd. *Plant Cell Physiol* 2014;**55**:2177−88.
28. Sun ZQ, Meng HL, Li J, Wang JF, Li Q, Wang Y, et al. Identification of novel knockout targets for improving terpenoids biosynthesis in *Saccharomyces cerevisiae*. *PLoS One* 2014;**9**:e112615.
29. Milne N, Thomsen P, Mølgaard Knudsen N, Rubaszka P, Kristensen M, Borodina I. Metabolic engineering of *Saccharomyces cerevisiae* for the *de novo* production of psilocybin and related tryptamine derivatives. *Metab Eng* 2020;**60**:25−36.
30. Zhao FL, Du YH, Bai P, Liu JJ, Lu WY, Yuan YJ. Enhancing *Saccharomyces cerevisiae* reactive oxygen species and ethanol stress tolerance for high-level production of protopanoxadiol. *Bioresour Technol* 2017;**227**:308−16.
31. Wang CX, Su XY, Sun MC, Zhang MT, Wu JJ, Xing JM, et al. Efficient production of glycyrrhetinic acid in metabolically engineered *Saccharomyces cerevisiae via* an integrated strategy. *Microb Cell Fact* 2019;**18**:95.
32. Engels B, Dahm P, Jennewein S. Metabolic engineering of taxadiene biosynthesis in yeast as a first step towards Taxol (Paclitaxel) production. *Metab Eng* 2008;**10**:201−6.
33. Li RS, Wang K, Wang D, Xu LP, Shi YS, Dai ZB, et al. Production of plant volatile terpenoids (rose oil) by yeast cell factories. *Green Chem* 2021;**23**:5088−96.
34. Wang QH, Liang L, Liu WC, Gong T, Chen JJ, Hou Q, et al. Enhancement of recombinant BmK AngM1 production in *Pichia pastoris* by regulating gene dosage, co-expressing with chaperones and fermenting in fed-batch mode. *J Asian Nat Prod Res* 2017;**19**:581−94.
35. Kim JE, Jang IS, Son SH, Ko YJ, Cho BK, Kim SC, et al. Tailoring the *Saccharomyces cerevisiae* endoplasmic reticulum for functional assembly of terpene synthesis pathway. *Metab Eng* 2019;**56**:50−9.
36. Wang D, Wang JH, Shi YS, Li RS, Fan FY, Huang Y, et al. Elucidation of the complete biosynthetic pathway of the main triterpene glycosylation products of *Panax notoginseng* using a synthetic biology platform. *Metab Eng* 2020;**61**:131−40.
37. Watanabe T, Tani M, Ishibashi Y, Endo I, Okino N, Ito M. Ergosteryl-β-glucosidase (Egh1) involved in sterylglucoside catabolism and vacuole formation in *Saccharomyces cerevisiae*. *Glycobiology* 2015;**25**:1079−89.
38. Li MJ, Kildegaard KR, Chen Y, Rodriguez A, Borodina I, Nielsen J. *De novo* production of resveratrol from glucose or ethanol by engineered *Saccharomyces cerevisiae*. *Metab Eng* 2015;**32**:1−11.
39. Dai ZB, Liu Y, Zhang XN, Shi MY, Wang BB, Wang D, et al. Metabolic engineering of *Saccharomyces cerevisiae* for production of ginsenosides. *Metab Eng* 2013;**20**:146−56.